CONCRETE LIBRARY OF JSCE NO.17, JUNE 1991

ANALYTICAL STUDY ON THE ULTIMATE DEFORMATION CAPACITY OF RC COLUMNS

(Reprinted from Transaction of JSCE, Vol.420/V-13, Aug. 1990)

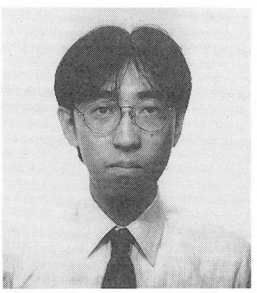

Hikaru NAKAMURA

Junichiro NIWA

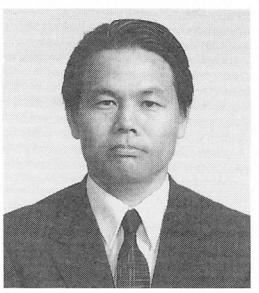

Tada-aki TANABE

SYNOPSIS

The finite displacement theory considering the effect of shear deformation is formulated. In this study, a computer program using the stiffness equation of reinforced concrete structures has been developed for the ultimate deformation analysis under cyclic loadings. Cyclic loading test of reinforced concrete columns under axial force was carried out and the applicability of this theory was investigated. The experimental values obtained from the specimens in which axial force, web reinforcement ratio and shear span and beam depth ratio were changed are compared with the calculated values. It is found possible to predict flexure or shear failure theoretically, when instability of structures is considered.

H.Nakamura is a Doctoral Student of Civil Engineering at Nagoya University, Nagoya, Japan. He received his Master of Engineering Degree from Nagoya University. His reserch interests include failure mecanism of RC stuctures. He is a member of JSCE and JCI.

J.Niwa is an Associate Professor of Civil Engineering at Nagoya University, Nagoya, Japan. He received his Doctor of Engineering Degree from University of Tokyo. His reserch interests include strength, deformation and design of reinforced concrete members under shear and torsion. He is a member of JSCE, JCI, IABSE and ACI.

T.Tanabe is a Professor of Civil Engineering at Nagoya University, Nagoya, Japan. He received his Doctor of Engineering Degree from the University of Tokyo. He is the chairman of JCI Comittee on the Thermal Stress of Massive Concrete Structures besides a member of various comittees of JSCE, JCI, and ACI. His main reserch is directed to the dynamic failure mechanism of RC structures besides the thermal stress.

---

1. Introduction

Seismic design of RC structures considers it essential that the seismic energy be absorbed by ductility after yielding of longitudinal reinforcement in structures. Therefore, prediction of the ultimate failure point and of the ultimate deformation capacity should be as accurate as possible. Many cyclic loading tests were carried out to predict the ultimate deformation capacity as well as the restoring force.[1][2] Several evaluation methods of the ductility are proposed on the basis of the results of experiments of the reinforced concrete members in Japan.[1][3] The methods to evaluate the ductility correctly, however, have not ever been established, since the ultimate behavior of reinforced concrete structures can be divided into a number of ways and it involves many factors in regard to material nonlinearities besides the factors of structural dimensions. The proposed methods based on experimental results are almost obtained from a small number of data and they do not have wide application for reinforced concrete structures.

To obtain results applicable for all RC structures, it is necessary to evaluate its complicated ultimate deformation behavior analytically. However, since analytical study in the past was almost based on the moment-curvature relation in a cross section, structural mechanism after yielding and effects on the ultimate deformation of many factors are not investigated in detail. Furthermore, these studies do not include the finite displacement effect by large axial force in which reinforced concrete structures lose their load carrying capacity due to the instability caused not only from softening of member stiffness but also from the finite displacement effect at the ultimate deformed state, and also do not include the structural instability and bifurcation problem, which may be important factors to predict the ultimate failure point.

The aim of this paper is to clarify analytically the behavior of reinforced concrete structures up to the ultimate deformed state. With these reasons, the finite displacement analysis has been performed, in which a layered beam element which includes shear deformations, is developed. The analytical results are compared with the cyclic loading tests of RC columns at Saitama University[14] and Nagoya University. Finally, it will be shown that the prediction of the ultimate failure point may be possible considering the instability of structures analytically.

2. Theoretical Consideration

(1) The Equation of Virtual Work for A Beam Element with Finite Displacements[4][5]

We confine our study within reinforced concrete columns which are comprised of beam-column elements. For the purpose of formulation based on finite element method, the following assumptions were made.

1) Variation of strain over the depth of an element is linear.

2) Bond slip between concrete and reinforcement can be neglected.

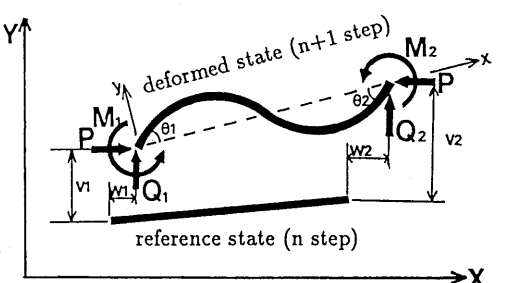

Fig.1 Beam Element

Fig.1 shows the deformation of a beam element subjected to axial force, shear force and bending moment at the end. To consider shear deformation, the displacement functions for x, y direction are expressed as

$$\begin{aligned} W(x,y) &= w - yv\prime_b \\ V(x,y) &= v_b + v_s \end{aligned} \tag{1}$$

where w is incremental axial deformation of deformed state, and v_b and v_s are incremental deformations of flexure and shear, respectively. The prime mark denotes the differentiation with respect to x direction. The axial and shear strains, ε_x and γ_{xy} , are related to the displacement functions for x, y direction for large displacement fields as shown in Eq(2).

$$\varepsilon_x = (w\prime - yv\prime\prime_b) + (v\prime_b + v\prime_s)^2/2$$
$$\gamma_{xy} = v\prime_s/2 \tag{2}$$

In Eq.(2), the term $w\prime^2$ is neglected since it is negligibly small compared with the other terms. We obtain then the equation of virtual work in the incremental form for a finite displacement problem as

$$\int_v \{\sigma_x \delta(w\prime - yv\prime\prime_b) + \tau_{xy}\delta v\prime_s\}dv + \int_v \{\sigma_x \delta(v\prime_b + v\prime_s)(v\prime_b^{(0)} + v\prime_s^{(0)})/2\}dv$$
$$+ \int_v \{\sigma_x^{(0)}\delta(v\prime_b + v\prime_s)^2/2\}dv + \int_s (f_x\delta u_x + f_y\delta u_y)ds = \delta W_r \tag{3}$$

$$\delta W_r = \int_s (f_x^{(0)}\delta u_x + f_y^{(0)}\delta u_y)ds - \int_v \{\sigma_x^{(0)}\delta(w\prime - yv\prime\prime_b) + \tau_{xy}^{(0)}\delta v\prime_s\}dv$$
$$- \int_v \{\sigma_x^{(0)}\delta(v\prime_b^{(0)} + v\prime_s^{(0)})(v\prime_b + v\prime_s)/2\}dv \tag{4}$$

where the terms with superscript (0) denote values in an arbitrary state of equilibrium in the reference state, and the others denote incremental values due to an additional load increment from the reference state. The higher order term, $\sigma_x\delta(v\prime_b + v\prime_s)^2$, has been neglected.

The first term in Eq.(3) is the variation of strain energy which corresponds to the linear displacement theory, that is, it represents the virtual work of perturbed stress due to the additional external force, and the second term represents the virtual work of additional stress with deformation, and the third term represents the virtual work of initial stress $\sigma_x^{(0)}$ as the reference state, while Eq.(4) is the virtual work of unbalanced force since the equilibrium in the previous load step is not satisfied strictly.

(2) Stiffness Equations

From the governing equation for bending, shear displacement of beam v_s is obtained as follows.

$$\frac{dv_s}{dx} = -\frac{1}{GA}\frac{dM}{dx}$$
$$= -\frac{EI}{GA}\frac{d^3v_b}{dx^3} \tag{5}$$

where GA is the shear stiffness of the effective cross section of reinforced concrete, and it depends on stress state or cracking.

By assuming a 3rd order polynomial for v_b and a linear equation for v_s and w, displacement function of each displacement increment can be obtained as

$$w = [N_u]\{du\}$$
$$v_b = [N_{vb}]\{dv\}$$
$$v_s = [N_{vs}]\{dv\} \tag{6}$$

$$N_u = [1 - \frac{x}{L}, \frac{x}{L}]$$
$$N_{vb} = [1 + \frac{6k}{L^2} - \frac{3}{L^2}x^2 + \frac{2}{L^3}x^3, -\frac{12k^2}{L^3} - \frac{4k}{L} + (\frac{12k}{L^2} + 1)x$$
$$+(-\frac{6k}{L^3} - \frac{2}{L})x^2 + \frac{1}{L^2}x^3, \frac{6k}{L^2} - \frac{3}{L^2}x^2 + \frac{2}{L^3}x^3,$$
$$\frac{12k^2}{L^3} - \frac{2k}{L} + (\frac{6k}{L^3} - \frac{1}{L})x^2 + \frac{1}{L^2}x^3]$$
$$N_{vs} = [\frac{6k}{L^2} - \frac{12k}{L^3}x, \frac{12k^2}{L^3} + \frac{4k}{L} - \frac{6k}{L^2}x, -\frac{6k}{L^2} + \frac{12k}{L^3}x, -\frac{12k^2}{L^3} + \frac{2k}{L} - \frac{6k}{L^2}x]$$

where the coefficient $k = (EI/GA)$ is the ratio of shear stiffness and flexural stiffness. When shear stiffness is infinite, displacement function reduces to the well-known function of a beam element.

The incremental displacement vectors $\{du\}, \{dv\}$ are shown by Eq.(7), respectively, where $w_i (i = 1, 2)$, $v_i (i = 1, 2)$ and $\theta_{bi} (i = 1, 2)$ denotes vertical, lateral displacements and bending rotation respectively.

$$\begin{aligned} \{du\}^T &= [w_1, w_2] \\ \{dv\}^T &= [v_1, \theta_{b1}, v_2, \theta_{b2}] \end{aligned} \tag{7}$$

Since shear rotations are dependent on bending rotations at the nodes of the element, the element has 6 degrees-of-freedoms i.e. axial, lateral displacements and bending rotations at the ends of the element.

Finally, we arrive at the following stiffness equation from Eq.(6) using Eq.(3) and Eq.(4).

$$([K] + [K_0] + [K_g])^{(n+1)}\{\Delta d\}^{(n+1)} = \{\Delta F\}^{(n+1)} + \{F_r\}^{(n)} \tag{8}$$

where K denotes the stiffness matrix, K_0 denotes the initial strain matrix, K_g denotes the geometric matrix which correspond to the each term of Eq.(3) and F_r is the unbalanced force vector which corresponds to Eq.(4). In the present solution method, the deformed configurations are accounted for by the coordinate transformations. Accordingly, matrix K_0 does not appear explicitly.[7]

(3) Stress-Strain Relation for Concrete under Cyclic Loadings

Stress-strain relation for concrete is shown in Fig.2(a). In zone of compression, stress-strain relation is represented by a second degree parabola with a linear falling branch. The slope for the falling branch, which is influenced by stirrup ratio and compressive strength of concrete, is determined by the Kent and Park model.[8] The stress-strain relation under cyclic loading is defined as follows. When the last maximum compressive strain ε_{max} is smaller than the axial strain corresponding to compressive strength ε_{C0}, stress is proportional to strain with a constant proportionality of $E_{C0} = 2f'_c/\varepsilon_{C0}$. And when ε_{max} is greater than ε_{C0} , stress is proportional with a constant proportionality of $2\sigma_{max}/\varepsilon_{max}$. In zone of tension, stress increases linearly with a constant proportionality of E_{C0} to tensile axial strength. And after that, it decreases linearly to the strain $10f_t/E_{C0}$.

Under cyclic loading, when stress varies from compression to tension crossing the $\sigma = 0$ axis, stress varies linearly towards to the tensile strength.[9] On the other hand, when stress varies from tension to compression, stress is equal to zero up to the strain at which stress has changed to tension from compression.

(4) Stress-Strain Relation for Reinforcement under Cyclic Loadings

Stress-strain relation for reinforcement is shown in Fig.2(b). Under monotonous loading, stress is proportional to strain with a constant proportionality of E_s to the yielding point, and increases linearly with a slope $E_s/100$ after that in both tension and compression zone.

Under cyclic loading, stress decreases linearly with a constant of E_s to the point $\sigma_s = 0$ and with $E_{B,i} (= -E_s log_{10}(\varepsilon_i - \varepsilon_y/6))$ (i denotes the cyclic number of times)[10] at reloading state until it will intersect the yielding curve.

(5) Slip of Longitudinal Reinforcement within a Footing

Lateral displacement caused by the slip of the longitudinal reinforcement of footing is not small compared to the total measured displacement. The slip of the longitudinal reinforcement is calculated by following procedure.

1) Strain distribution of a longitudinal reinforcement in the footing, which is illustrated in Fig.3, is assumed before and after yielding. Here, l_e denotes the length of region where elastic strain is induced before yielding of a bar, while l_{ey} denotes the length of the elastic region after yielding of a bar and l_p denotes the region where plastic strain is induced after yielding of a bar.

2) Bond stress in post-yield range is not much larger than that in elastic range and it decreases suddenly with yielding of reinforcement[12]. Bond stress and strain relation is shown in Fig.4, in which the curve is determined considering the experimental results[11][12].

3) The length where tensile stress occurs is determined so as to satisfy the equilibrium condition between bond stress along the reinforcement in the footing and the stress of reinforcement at the top of the footing. Here, the bond stress in the area of l_e is balanced with the elastic stress of reinforcement and in the area of l_p, and it is balanced with the stress increment after yielding.

4) Slip of a longitudinal reinforcement(Δ) can be represented by integration of strain distribution, which is obtained from the equilibrium condition, along the reinforcement. The displacement influenced by the slip at the top of the column is calculated from Eq.(9) and Eq.(10).

$$\theta = \Delta / x \tag{9}$$

$$\delta_1 = h\theta = h\Delta / x \tag{10}$$

where, x denotes the distance from neutral axis to a longitudinal reinforcement in a cross section at the bottom of column and h denotes the length of the column.

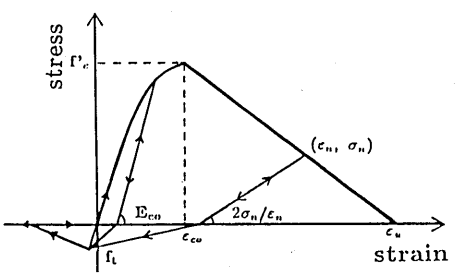

Fig.2(a) Stress-Strain Relation for Concrete

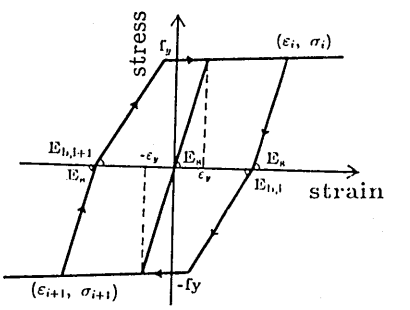

Fig.2(b) Stress-Strain Relation for Reinforcement

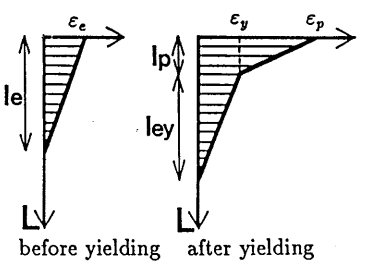

Fig.3 Strain Distribution of Reinforcement in Footing

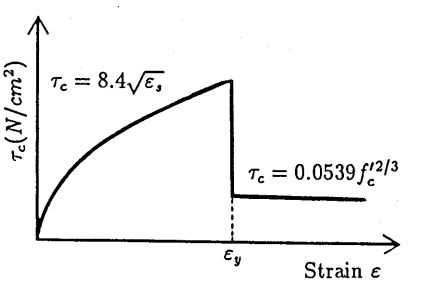

Fig.4 Bond Stress- Strain Relation

It is considered that the slip of reinforcement, in general, contributes to the geometric nonlinearities of the structure. However, in this paper the displacement due to slip is not included in the consideration of secondary effect of geometrical nonlinearity.

(6) Calculation Method

A computer program is developed according to the previous discussion. Since the stress and Young's modulus vary with the depth of the element, an element is subdivided into a number of layers(Fig.5). Integration in each term of Eq.(8) can be represented by the sum of the amount in each subdivided element in which material nonlinearlity is assumed[13]. Young's modulus used in stress-strain relation for each layer is the tangent modulus. Material nonlinearlity and cracking of concrete are thus considered accurately.

Representative expression of a stiffness term is given using a component K_{22} which contains the contribution of shear displacement.

$$K_{22} = \sum_{i=1}^{ELM}\sum_{j=1}^{m}\frac{EI(j)}{L^6(1+T_j)^2}\{(36L_i^2+144k_j)(r_{j+1}-rj) -72L_i(r_{j+1}^2-r_j^2)+48(r_{j+1}^3-r_j^3)\} \quad (11)$$

$$EI(j) = \sum_{k=1}^{m} E(i,j,k)b_k(q_{k+1}^3-q_k^3)/3 \quad (12)$$

$$T(j) = 12k(j)/L_i^2 \quad (13)$$

$$k(j) = \sum_{k=1}^{n}\frac{1}{GA(j)}E(i,j,k)b(k)\{(q_{k+1}^3-q_k^3)/3+y_0(q_{k+1}^2-q_k^2)+y_0^2(q_{k+1}-q_k)\} \quad (14)$$

where y_0 is the distance from neutral axis to central axis in the cross section.

Young's modulus in each layers are obtained considering the strain distribution in the cross section, and flexural stiffness is calculated to multiply them by the geometrical moment of inertia for the central axis. This procedure is repeated for all subdivided layers, and their summation represents the accurate flexural stiffness $EI(j)$ at each cross section as given in Eq(12). The component of stiffness matrix in an element can be obtained by summing up the flexural stiffness at each cross section to the x direction(Eq(11)). Here, shear stiffness $GA(j)$ is determined at each cross section.

As the configuration changes for large displacement, the neutral axis moves within the reinforced concrete members. So, it is necessary to satisfy the condition that the axis line coincides with x direction. For the purpose, the geometrical moment of inertia is calculated around the central axis in the cross section and the change of the neutral axis is considered by change of geometrical moment of area.

In the analysis, stiffness equations are solved iteratively to compute displacement increments with Newton-Raphson Method. The analysis was performed by updating stiffness matrix at every load step within each step until the norm of unbalanced forces relative to applied force becomes stationary. In every step, the eigenvalues and the eigen modes of updated effective stiffness matrix are searched for. Structural instability is investigated by the occurrence negative eigenvalues and the numerically obtained displacement vector is compared with eigen modes of updated effective stiffness matrix in each step.

3. Experimental Verification

(1) Cyclic Loading Test of Nagoya University

A cyclic loading test of reinforced concrete slender columns under constant axial force was carried out in order to investigate instability effects by large axial force.

(a) Specimen

The dimension of a specimen is shown in Fig.7. The specimen has an "I" shape cross section with length of 100(cm) and a depth and shear span ratio of 12.5. Longitudinal reinforcements $D3 \times 6$ are arranged and web reinforcements, which have an area of cross section of 0.0078(cm^2), are arranged with spacing of 4(cm). The longitudinal reinforcement ratio is 0.67(%) and the web reinforcement ratio is 0.45(%).

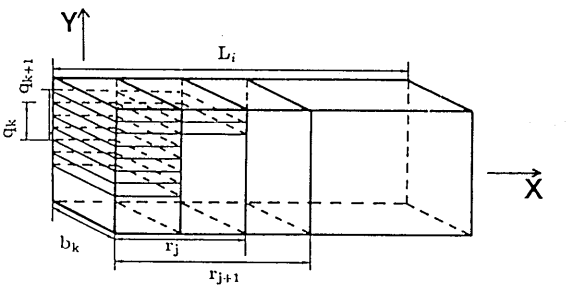

Fig.5 Subdivided Element

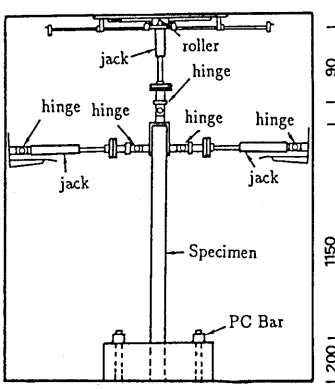

Fig.6 Loading Apparatus

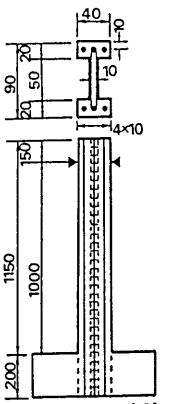

Fig.7 Dimension of Slender RC Column(Nagoya Univ.)

The properties of material used in a specimen is given in Table-1. The maximum compressive strength of concrete is 30.50(N/mm^2). A longitudinal reinforcement has 24.12(KN/cm^2) of tensile yielding stress. Stress-strain relationship of a deformed longitudinal reinforcement(D3) is shown in Fig.8 with circle and the relation used in the analysis is shown with a solid line.

(b) Loading

The loading apparatus is shown in Fig.6. A specimen was subjected to shear force at the top by a horizontal jack with constant axial load(4000N). The condition that axial load must be perpendicular to the ground is satisfied by moving a jack, which is moved using a roller in the same distance as the lateral displacement occurred at the top of the column.

The loading is carried out by controlling lateral displacement with graduation of 0.005, 0.01, 0.015, 0.03, 0.06, and 0.09 for rotational angle of a member in every cycle.

(c) Test Results and Discussion

The experimental lateral load versus lateral displacement relations are shown by a solid line in Fig.9. A large displacement which is accompanied by cracking and yielding of reinforcement defined as the ratio of lateral displacement (δ) to the length of the member (L) is observed to exceed the value of 0.1. The ultimate state is achieved by buckling of reinforcement. The analytical result is shown with a broken line in Fig.9. A good agreement between experimental and computed values can be seen up until the final state for which δ/L is about 0.1.

Fig.10 shows skeleton curve of experimental and computed values under monotonous loading. The solid line corresponds to the results of finite displacement theory while the broken line corresponds to the results of linear displacement theory. The RC members, which have large displacement and significant axial force, showed notable influence of $P-\Delta$ effect. This experimental value can be represented accurately by finite displacement theory while linear

displacement theory can not.

The point D in Fig.10 corresponds to a point that gives rise to the second negative eigen value of tangent stiffness matrix of structures. After that point, structures become unstable and the loading capacity falls rapidly. It is considered that axial force can not be sustained after the point D.

(2) Cyclic Loading Test of Saitama University[14]

The specimens used in a cyclic loading test of Saitama University, which is shown in Fig.11, have a cross section($20 \times 15(cm)$) size of practical use. Therefore, the applicability of the analysis was also investigated to the test results of Saitama University in which axial force, web reinforcement ratio and shear span and beam depth ratio were changed. The analysis is performed under monotonous loading and computed value is compared with the skeleton curve of experimental value.

The material properties used in the analysis are given in Table-2. The loading was carried out with the same incremental displacement steps of $\pm\delta_y$ (displacement corresponding to the yielding load), $\pm 2\delta_y$, $\pm 3\delta_y$, $\cdots$, to failure in ten cycles.

(a) Effect of Axial Force(σ_0)

It seems that the axial stress is one of the most influential factors for ductility of reinforced concrete columns. The solid lines in Fig.12 show the skeleton curve of experimental values with axial stress(σ_0) of 0 and 200(N/cm^2). The computed values are shown in Fig.12 with broken lines. The difference between experimental and computed values increases after the maximum load carrying capacity. The reason why computed value over estimates the experimental values is explained later. However, the applicability of the analysis to predict effect of axial force seems reasonable since the difference between the two is not significant.

Table-1. Material Properties

Reinforcement		Concrete	
Es (MN/cm^2)	fy (KN/cm^2)	Ec (MN/cm^2)	f'c (KN/cm^2)
16.0	24.12	2.05	3.05

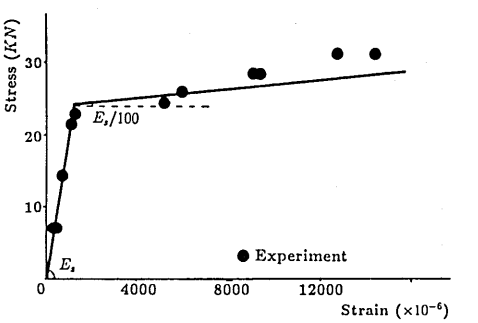

Fig.8 Stress-Strain Relation of Reinforcement(D3)

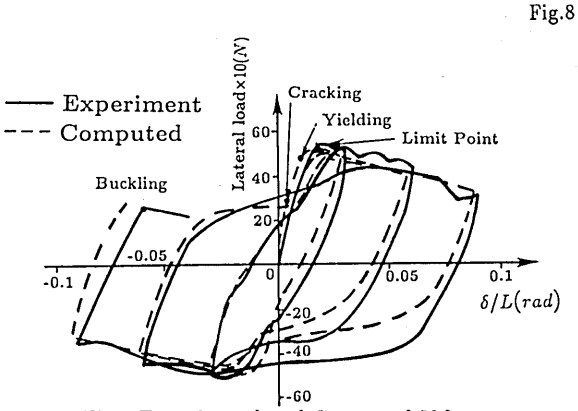

Fig.9 Experimenal and Computed Value

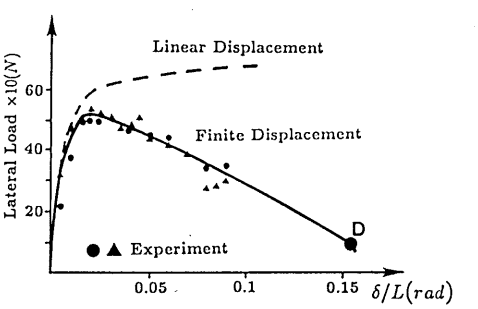

Fig.10 Skelton Curve and Computed Value

(b) Effect of Web Reinforcement Ratio(ρ_w)

The lateral load-lateral displacement relation affected by web reinforcement ratio are shown in Fig.13 with solid lines. The web reinforcement ratio were 0.077, 0.12, 0.23(%). The results of analysis are illustrated in Fig.13 with the broken lines for each ratio.

The effect of web reinforcement ratio is taken into consideration by varying the slope of a falling branch for concrete using Kent and Park model. The restrainting effect of web reinforcement mainly cause the maximum compressive strength of concrete to increase and the slope of a falling branch to be flatten. In the analysis, the latter effect only is considered. Hence, the lateral load at the yielding is different from the values of experiment and the analytical result is the same until the concrete stress moves into a falling branch. In either case the analytical results, however, show a good agreement with experimental results for effect of web reinforcement ratio to the ultimate deformed state.

Table-2. Material Properties

Concrete			Reinforcement	
f'c (KN/cm^2)	ft (KN/cm^2)	ε_{c0}	fy (KN/cm^2)	ε_y
3.0	0.6	3000×10^{-6}	40.0	2500×10^{-6}

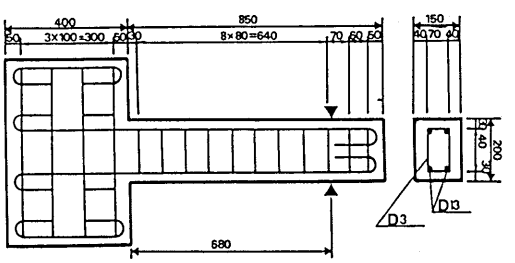

Fig.11 Dimension of RC Column(Saitama Univ.)

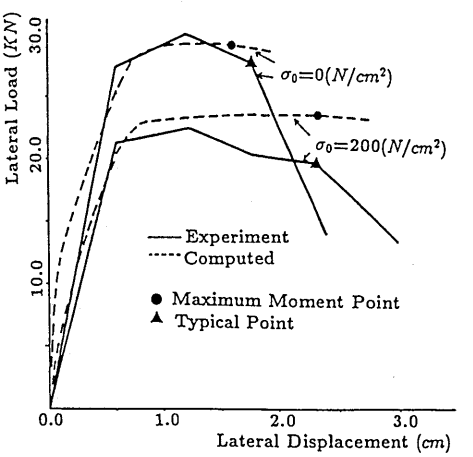

Fig.12 Effect on Axial Stress(σ_0)

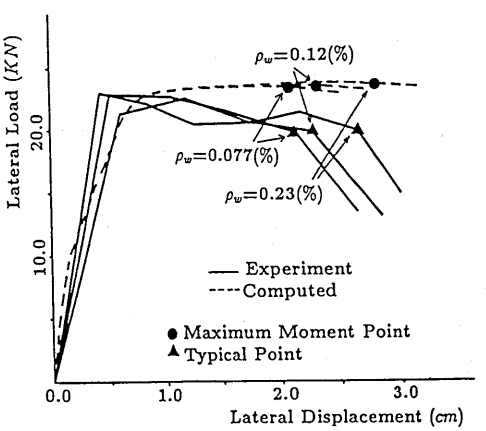

Fig.13 Effect on Web Reinforcement Ratio(ρ_w)

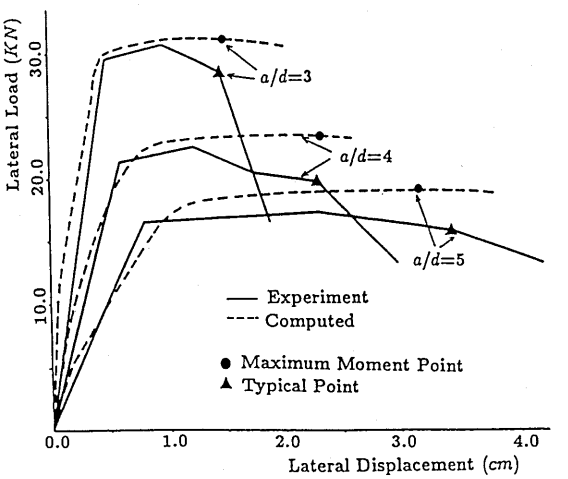

Fig.14 Effct on Shear Span and Beam Depth Ratio(a/d)

(c) Effect of Shear Span and Beam Depth Ratio(a/d)

The effect of length of column was investigated with zero axial stress and the constant web reinforcement ratio of 0.12(%). The three cases ($a/d = 3.0, 4.0, 5.0$) were investigated. Fig.14 shows the skeleton curves of experimental and the computed values. The solid line and the broken line corresponds to the result of experiment and analysis, respectively. Load carrying capacity tends to be larger and ductility tends to be smaller with decreasing the shear span and beam depth ratio in experiments. The analytical results represent this effect accurately.

4. Characteristic Point for Ductility of RC Column

Ductility ratio is defined by Machida et al.[1] as shown in Eq.(15) based on the experimental result.

$$\mu = \delta_{80max}/\delta_y \tag{15}$$

where δ_{80max} is the lateral displacement corresponding to the load of 80% of the maximum load carrying capacity and δ_y is the lateral displacement when longitudinal reinforcement yields in member. His definition is considered to be based on the fact that the restoring force often decrease rapidly at the lateral displacement corresponding to the load of 80% in cyclic loadings. This is confirmed that the lateral loads decrease rapidly at those point in Fig.12, Fig.13 and Fig.14.

However, in this analysis the characteristic point to define ductility is identified as the maximum moment point of the analytical results. The maximum moment is the sum of the moment from the lateral load and the moment introduced by the $P-\Delta$ effect. The maximum moment point obtained by analysis is shown by the mark "•", and the characteristic points in experiment are shown by the mark "Δ" in Fig.12, Fig.13 and Fig.14. It is seen from these figures that the points coincide with the characteristic points in experiment for every factors. Table-3 shows the results for each case. Hence, it may be reasonable to define the ductility of RC members by Eq.(16). In other words, ductility should be defined by the ratio of the ultimate displacement corresponding to the maximum moment point (δM_{max}) and the lateral displacement corresponding to the yielding (δ_y).

$$\mu = \delta M_{max}/\delta_y \tag{16}$$

When the cyclic loading is carried out after the yielding of reinforcement, there is a specific displacement point beyond which the restoring force decreases with repeated loadings. This is the special character of the failure of the cyclic loadings, which is different from the monotonous loadings. The characteristic point corresponds to the point that the load carrying capacity decreases rapidly and before the characteristic point the decrease of restoring force is small in

Table-3. Results of Analysis

ρ_w (%)	a/d	σ	δy (cm)	δyc (cm)	$\delta y/\delta yc$	$\delta_1/\delta yc$	Qy (KN)	Qyc (KN)	Qy/Qyc	δu (cm)	δuc (cm)	$\delta u/\delta uc$	$\delta_1/\delta uc$
0.12	4.0	0	0.6	0.69	0.87	0.511	21.3	21.9	0.97	2.29	2.31	0.99	0.516
0.12	4.0	20	0.6	0.73	0.82	0.536	27.4	28.1	0.97	1.77	1.57	1.13	0.470
0.077	4.0	0	0.51	0.69	0.74	0.511	22.8	21.9	1.04	2.13	2.09	1.02	0.502
0.23	4.0	0	0.43	0.69	0.62	0.511	23.0	21.9	1.05	2.64	2.79	0.95	0.542
0.12	3.0	0	0.5	0.46	1.08	0.584	29.5	29.8	0.99	1.45	1.49	0.97	0.583
0.12	5.0	0	0.8	0.96	0.83	0.469	16.5	17.0	0.97	3.45	3.17	1.09	0.457

a cycle. As mentioned above, the displacement corresponding to the maximum moment obtained from the analysis under the monotonous loading is found to be in good agreement with this characteristic point. One reason for the fact is considered that concrete in compression zone moves into the falling branch of stress-strain relation after the maximum moment point is reached. That is, it is considered that beyond this point resistance of concrete decreases in every cycle and load carrying capacity of member decreases, the concrete cover spalls, and finally shear deformation increases rapidly in a cycle if the loading is carried out in this range.

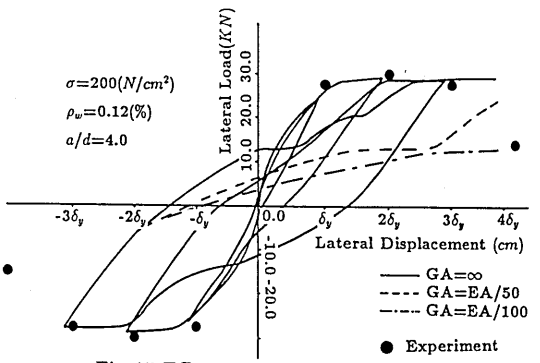

Fig.15 Effect on Shear Deformation

The effect of the shear deformation is investigated analytically to give some values of shear stiffness(GA) for the specimen of Saitama University. Fig.15 shows the analytical results for the effect of shear deformation. The shear stiffness are changed to three cases in a cycle of $3\delta_y$, when the concrete of the bottom of column does not contribute to the stiffness, that is only reinforcement at the bottom sustain the specimen. The solid line shows the results for the case where GA is infinite and the broken line is the results when GA is $EA/50$ and the dash line corresponds to the result when GA is $EA/100$. As shear stiffness is applied to small values, the effect of shear deformation increases and the load carrying capacity at any displacement tends to be small relatively. It will be expected that the lateral load decreases gradually with the broken line and the dashed line in cycle of $4\delta_y$.

5. Ductility and Instability for RC Column

It can be considered that the instability characteristic is effective to define the failure of the structure. An equilibrium state is called stable if response to a vanishingly small disturbance also remains vanishingly small[15].

The condition for the state of stable equilibrium under load is stated that the determinant of updated effective stiffness matrix is positive,

$$det(K_e) > 0 \tag{17}$$

where $K_e = K + K_0 + K_g$ is the effective stiffness matrix for structures. For the critical state of neutral equilibrium

$$det(K_e) = 0 \tag{18}$$

Eq(18) implies that at least one eigenvalue is zero. Accordingly, unstable structural behavior is defined by existence of negative eigenvalues. The definition in which the structure is either stable or unstable can be easily determined by using the eigenvalue analysis. It should be noted, however, that there exist two possible interpretations for the state for which the negative eigenvalues emerged. One is the state which continues after the limit point, and the other is the state which continues after the bifurcation point. Analytical example of the limit point, in which the load becomes stationary, is the maximum load point in the load-displacement relation. We are able to get one equilibrium path beyond the limit point analytically, if the displacement is controlled. After the emergence of the bifurcation point, however, there exist alternative equilibrium states which can be reached with some kinematically admissible displacement vector.

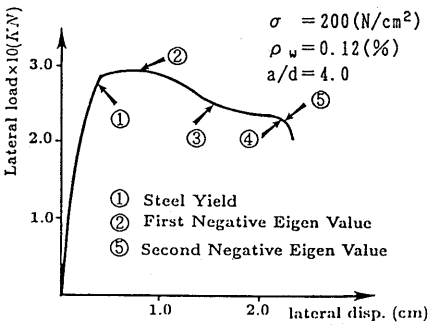

Fig.16 Load-displacement Relation for GA Is Infinite

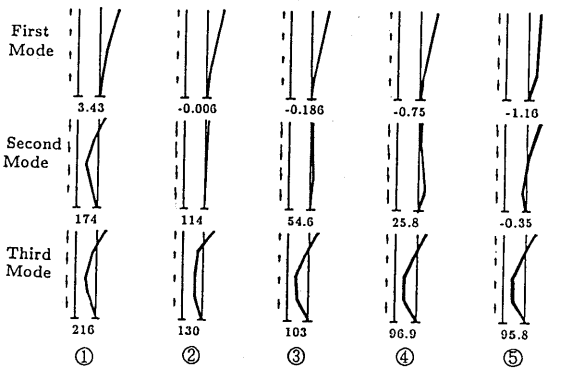

Fig.17 Eigen Modes and Eigenvalues for Each Load Step

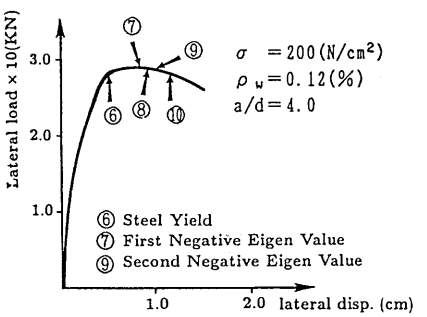

Fig.18 Load-Displacement Relation for GA Is Variable

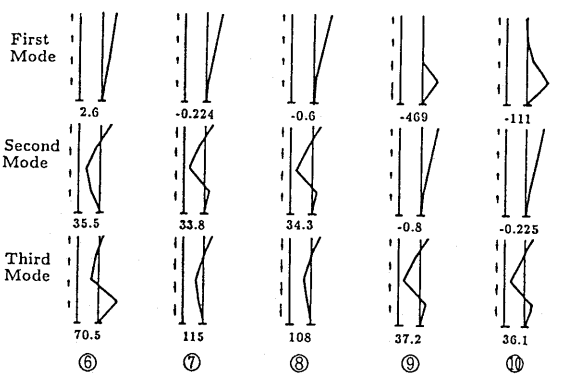

Fig.19 Eigen Modes and Eigenvalues for Each Load Step

This fact implies that it is important to know the equilibrium path which is followed by the structure.

We investigated the instability behavior for two cases. The first case considers only flexural deformation and the second case considers the flexural and shear deformations for RC column. The RC column analyzed is a test specimen of Saitama University with the axial stress(σ_0) of 200(N/cm^2), web reinforcement ratio(ρ_w) of 0.12(%) and the shear span of 4.

For the first case in which shear stiffness (GA) is infinite, the relation between lateral load and lateral displacement under monotonous loading is shown in Fig.16. The eigenvalues and the eigen modes of tangential stiffness matrix for each load level, which correspond to 1-5 in Fig.16, are shown in Fig.17. The analytical result yields a negative value for the lowest eigenvalue when the load level is 2. But the eigen modes are almost the same in comparison with the previous step. It is considered that this point corresponds to the limit point. As expected, the load carrying capacity decreases accordingly as lateral displacement increases after this point as shown in Fig.16. The structure is in a state of unstable equilibrium if the lateral load is controlled. In such a case, since structures can still support an axial force, structures do not necessarily collapse. Moreover, this eigen mode is kept unchanged until the second negative eigenvalue is initiated. When load level is 5, second eigenvalue becomes negative and lateral load decreases rapidly and the lowest eigen mode differs from the one of previous load step. This point corresponds to the bifurcation point. In this mode, the rotation angle at the bot-

tom and the axial deformations becomes very large. It is considered that structures can not practically support axial force at that point.

Secondly, we investigated the case which considers both flexural and shear deformations. The influence of shear deformation is considered with shear stiffness(GA) of a cross section which varies with the variation of n

$$GA = \frac{\rho_w j d b_w E_s}{4n\rho_w + 1} \tag{19}$$

where ρ_w ; stirrup ratio, jd ; the distance between compression stress and tensile stress, b_w ; width of the cross section, $n = E_s/E_c$, E_s ; the Young's modulus of stirrup, and E_c is the Young's modulus of concrete which is averaged through the cross section. Eq(19) is the shear stiffness which is obtained by Truss analogy. The results are shown in Fig.18. The eigenvalues and eigen modes for each load level are shown in Fig.19. When the load level is the one denoted by 9, which is almost equal in level to the maximum point, the second eigenvalue becomes negative and eigen mode changes suddenly. Emergence of the mode is much earlier than in the previous case. Obviously, this is due to the shear deformation effect. If more suitable shear stiffness is used, the prediction for shear failure may be possible using the analytical method. Though the numerical solution corresponding to the lowest eigenvalue is considered to give much lower horizontal resistance, the lateral load does not decrease rapidly as shown in Fig.18, since the numerical procedure took the fundamental path.

6. Conclusion

To investigate the ultimate deformation capacity of RC structures, the finite displacement formulation considering the shear deformation was carried out and the instability analysis is combined. A computer program was developed, in which the cracking of concrete and the nonlinear stress-strain relation of material was considered accurately, for the ultimate deformation analysis. And experiment using a RC slender column under axial and horizontal forces has been performed for large displacements having rotation angle of the column of over 0.1. Comparison with the experimental result of cyclic loading test with the analysis shows applicability of the analysis method. Moreover, it was shown that the effects on the ductility for the reinforced concrete column of axial force, web reinforcement ratio and shear span can be represented reasonably in this analysis using the results of cyclic loading test of Saitama University. Then, it was shown that the maximum moment point is an reasonable characteristic point to define the ductility in the analysis.

Instability analysis combined with the large displacement analysis indicated that the ultimate deformed state is closely defined by the emergence of the bifurcation point in the structural stiffness matrix for which the finite displacement is taken account of. Moreover, in the analysis , it is suggested that the shear failure is also predictable by the instability analysis.

Reference

[1] Machida, A., Mutsuyoshi, H. and Toyoda, K.: Evaluation of Ductility of Reinforced Concrete Members, Proc.JSCE, No.378, pp.203-212, 1987.
[2] Ozaka, Y., Suzuki, M., Kuwazawa, S. and Ishibashi, T.: Load-Deflection Characteristics of Reinforced Concrete Columns under Static Alternating Cyclic Loads, Proc.JSCE, No.372, pp.45-54, 1986.
[3] Ohta, M.: An Experimental Study on the Behavior of Reinforced Concrete Bridge Piers under Cyclic Loadings, Proc.JSCE, No.292, pp.65-74, 1978.
[4] Kawai, T.: Analysis for Buckling Theory, Baifukan, 1970.
[5] Nakamura, H. and Tanabe, T.: Ductility and Stability of RC Structures by Finite Displacement Theory, JCI Colloquium on Ductility of Concrete Structures and It's Evaluation,

pp.153-162, March, 1988(in Japanese)
[6] Hasegawa, A., Iwakuma, T. and Kuranishi, S.: A Linerized Timoshenko Beam Theory in Finite Displacements, Proc.JSCE, Structural Eng./Earthquake Eng., Vol.2, No.2, October 1985.
[7] Cook, Robert D.: Concepts and Applications of Finite Element Analysis, 2nd ed. New York, Wiley, 1981.
[8] Kent, D.C. and Park, R.: Flexural Members with Confined Concrete, Proceedings of ASCE, Vol.97, No.ST7, pp.1969-1990, July 1971.
[9] William, K. J., Bicanic, N. and Sture, S.: Constitutive and Computational Aspects of Strain-softening and Localization in Solids, ASME/WAN 84 meeting, New Orleans, Symposium on Constitutive Equations, Marco and Computational Aspects, ASME Vol.G00274, ed.K.William, New York 1984.
[10] Matsumoto, K.: Analytical Study on Moment-Curvature Relationship for Ductility Design of RC Bridges, Doctor Degree of Nagoya Univ., 1985.
[11] Miyatake, T. and Kubota, T.: Study on the Reinforced Concrete Column, 33th Annual Conference of Architectural Institute of Japan, 1960.
[12] Shima, H., Chou, L. and Okamura, H.: Bond Characteristics in Post-Yielding Range of Deformed bars, Proc.JSCE, No.378, pp.213-222, 1987.
[13] Umehara, H., Tanabe, T. and Yoshida, K.: A Study on Behavior of a Partially Bonded Prestressed Concrete Rigid Frame under Lateral Loading, Proc.JSCE, No.378, pp.89-98, 1988.
[14] Toyoda, K., Mutsuyoshi, H. and Machida, A.: Evaluation of Ultimated Deflection of RC Members, Proc.JCI, No.7, pp.629-632,1985.
[15] Hill, R.: A General Theory of Uniqueness and Stability in Elastic-Plastic Solids, J.Mech.Phys. Solids, 6, pp.236-249, 1958